

SUMMARY OF FLIGHT TESTS OF AN AIRBORNE LIGHTNING  
LOCATOR SYSTEM AND COMPARISON WITH GROUND-BASED  
MEASUREMENTS OF PRECIPITATION AND TURBULENCE

Bruce D. Fisher and Norman L. Crabill  
Langley Research Center

SUMMARY

The National Aeronautics and Space Administration is conducting research involving the operation of aircraft in and around thunderstorms. The tests described herein were conducted at the National Severe Storms Laboratory of the National Oceanic and Atmospheric Administration, in Norman, Oklahoma, during May 1978, and at the NASA Wallops Flight Center, in August 1978, using a NASA-owned twin-engine light transport aircraft. This paper includes data from an airborne lightning locator system and data relating to storm intensity obtained by the NSSL ground-based Doppler radars and the NASA Wallops SPANDAR radar. When comparing lightning locations from the airborne lightning locator system with ground-based Doppler radar measurements of reflectivity and spectrum width, the lightning locations tended to be further from the aircraft position than the Doppler radar contours, but at the same relative bearing from the aircraft as the Doppler radar contours. The results have also shown that some convective storms generate little or no lightning for a significant part of their life cycle, but can produce at least moderate turbulence. Therefore, a lack of lightning activity cannot be accepted as an inference of a corresponding lack of other hazards to the flight of aircraft through convective storms.

INTRODUCTION

Although there have been significant advances in ground-based and airborne equipment for providing information relative to severe weather, there continues to be a serious aviation safety problem associated with aircraft operations in the vicinity of severe storms. One of the problems is that of providing the pilot with information needed to avoid storm hazards which exceed the design capabilities of the airplane and its systems. As part of NASA's aviation safety research program, NASA Langley Research Center has undertaken a storm hazards research program to extend the knowledge and understanding of atmospheric processes as they affect aircraft design and operations.

The initial phase of this program, conducted during the storm season of 1978 at NSSL and NASA Wallops Flight Center, involved the preliminary

evaluation of instrumentation and operational procedures around the periphery of storms using a NASA-owned twin-engine light transport aircraft. The aircraft was equipped with a commercially available lightning locator system, which was tested to determine the ability of the device to detect and locate lightning discharges, and to develop an understanding of how the device should best be used to avoid hazardous weather in flight operations. The data recorded during this program included data from the airborne lightning locator system and contours of precipitation reflectivity and radial velocity spectrum width (turbulence) from ground-based weather radars. This paper presents the results of the comparison between airborne indications of lightning and other measurements of storm hazards.

## TEST EQUIPMENT AND PROCEDURES

### NASA Aircraft

Physical characteristics.- The NASA test airplane was a twin-engine, high-wing, light STOL-type transport. The maximum design gross weight was 48 928 N (11 000 lb) and the aircraft weight ranged between 38 253 and 45 370 N (8 600 and 10 200 lb) during these tests. A dimensioned three-view drawing of the aircraft is given in figure 1.

Data acquisition.- Thirty-six parameters were recorded by the onboard data system. The parameters included angle of attack, angle of sideslip, static pressure, total pressure, altitude, altitude rate, total temperature, accelerations in three body axis, impact pressure, and the output of an airborne lightning-locator device. The data system included an Inertial Navigation System (INS). The following parameters from the INS were recorded: pitch, roll, and heading attitude, latitude and longitude, drift angle, crab angle, and an inertially-derived vertical acceleration.

The parameters from the INS were digitally recorded in a 16-bit stream at 20 samples/sec. The memory of the lightning locator system was sampled and recorded by the onboard data recording system 30 times/sec. Although the airborne lightning locator system was operated continually, the data were only recorded when the onboard data system was operating. The other parameters were recorded on the magnetic tape data system at 80 samples/sec by a pulse-code modulation method. All data were correlated with a time code.

Airborne lightning locator system.- As a part of these tests, a commercially available device for indicating the position of lightning strikes relative to the aircraft was installed. The device consists of a detector unit connected to an ADF antenna, a control unit, and a 7.5 cm (3-inch) diameter CRT display. The control box and display unit are shown in figure 2 as installed in the co-pilot's instrument panel. The device determines lightning location by radio direction finding on spherics and determining a line of position. The range from the aircraft along the line of position is determined by comparing the received signal wave shape and

strength with an assumed lightning model. The position of the lightning is presented as a dot on the CRT. If the lightning is very intense, or very close, the device will present a series of dots along the line of position. This characteristic is known as "radial spread."

The line of position and location of the lightning strike is determined relative to the airplane position and heading at the time of the lightning strike. Thus, over a period of time, particularly with airplane heading changes, the existing CRT display of previously stored lightning locations does not represent their location relative to the new airplane position and heading. The CRT display can be erased and the indications of the lightning locations removed from the system memory by depressing the "clear" function button on the control unit. The memory section can store the location of 128 lightning signals between manual clearing of the unit. After this number of signals is recorded, additional signals overwrite the memory by replacing the oldest values with the newest. This often occurs in very electrically-active storms.

The signals used to generate the CRT display were recorded on the magnetic tape data system. Also, a video recorder was installed to record the CRT presentation. The center of the CRT is the aircraft location with a 360° azimuth presentation of lightning about the aircraft (figure 2). Two concentric rings about the airplane symbol represent various ranges up to 40, 100, or 200 n.mi., depending upon the position of the range selector switches on the control unit. The range setting was manually recorded by the test operator.

Transformation of lightning locations to true geographic positions.-  
Each lightning event detected by the airborne lightning locator in the NASA aircraft was stored by the locator system as a number pair representing the longitudinal and lateral position of the event with respect to the aircraft location at the time of the event. The memory of the system was subdivided into a 63 x 63 rectangular grid for spatially locating each lightning event. This spatial presentation was superimposed on the CRT display in the cockpit (see figure 2), with the lower left-hand corner of the display being the (1,1) matrix position, and the upper right-hand corner being the (62,62) position. Up to 128 individual lightning events could be stored and displayed by the system. After 128 points had entered the system, the new points began replacing the old points in sequential order.

For data reduction, the contents of the memory of the airborne lightning locator, and, hence, the CRT display, were digitized for the selected times of interest. The lightning rate of production for the locator was computed at 30-sec intervals after the flight. Centered on the 30-sec interval times, a program counted the number of changes in the lightning locator's memory for ±15 seconds. The number of changes counted in each interval were then divided by time to give a normalized value equivalent to the lightning rate of production in events/sec. When necessary, the sample counting intervals were shortened to eliminate changes associated with the crew manually clearing the memory. When this occurred, the shorter time interval was used

for normalization. The 30-sec interval procedure was automatically interrupted in the program whenever there was a break in the data, either from turning the data recorder on and off, or from clearing the locator memory. In these instances, computations were made for +15 secs from the time the first new data appeared on tape. Subsequent computations were then made at 30-sec intervals, using this new first time as a new starting point. Every time a computation was made, the contents of the memory (and CRT) were plotted on computer drawn replicas of the CRT grid to produce a record of the lightning scenario presented to the crew by the airborne lightning locator system.

Although the basic lightning locator data used for the cockpit display were not updated for changes in aircraft position and heading, these data, in conjunction with the INS airplane position data, allowed the measured lightning locations for the reduced data to be resolved relative to fixed ground coordinates throughout time intervals of interest. For the Oklahoma flights, the transformations were made between those times corresponding to the start and stop times of the NSSL Doppler radar sample intervals. For the single flight in the vicinity of NASA Wallops, the transformations were made for the full length of the aircraft data run.

The transformation of the recorded number pairs, representing the lightning locations, to geographical locations was a five-step process: (a) conversion of the number pairs into longitudinal and lateral distances with respect to the aircraft; (b) converting the distances in step (a) into a radial and angular displacement from the aircraft; (c) computation of the angular displacement of the point from true north; (d) computation of the aircraft position with respect to the ground-based radar; and (e) transformation of the lightning point into coordinates with respect to the ground-based radar. The transformation equations used were:

For  $X' > 0$

$$X_{ns} = \{(X')^2 + (Y')^2\} \sin \{90^\circ - \tan^{-1} (Y'/X') + \Psi\} + X_{ac} \text{ and}$$

$$Y_{ew} = \{(X')^2 + (Y')^2\}^{\frac{1}{2}} \cos \{90^\circ - \tan^{-1} (Y'/X') + \Psi\} + Y_{ac}$$

and for  $X' < 0$

$$X_{ns} = \{(X')^2 + (Y')^2\}^{\frac{1}{2}} \sin \{270^\circ - \tan^{-1} (Y'/X') + \Psi\} + X_{ac} \text{ and}$$

$$Y_{ew} = \{(X')^2 + (Y')^2\}^{\frac{1}{2}} \sin \{270^\circ - \tan^{-1} (Y'/X') + \Psi\} + Y_{ac}$$

where:

$X_{ns}$  is the north-south distance of the lightning point from a ground-based radar, positive north (km)

- $Y_{ew}$  is the east-west distance of the lightning point from a ground-based radar, positive east (km)
- $X'$  is the longitudinal distance of the lightning point from the aircraft, positive ahead (km)
- $Y'$  is the lateral distance of the lightning point from the aircraft, positive to the right (km)
- $\Psi$  is the true heading of the aircraft from the INS (deg)
- $X_{ac}$  is the north-south distance of the aircraft from a ground-based radar, positive north (km)
- $Y_{ac}$  is the east-west distance of the aircraft from a ground-based radar, positive east (km).

During calibration, it was found that the actual center of the lightning locator display and memory, which represents the aircraft position, was offset from the presumed center, and varied with the range selected. The center offsets and scale factors were used to compute  $X'$  and  $Y'$  using the equations:

$$X' = (X \text{ value in memory} - X \text{ center offset}) \times (\text{scale factor})$$

$$Y' = (Y \text{ value in memory} - Y \text{ center offset}) \times (\text{scale factor})$$

The aircraft position ( $X_{ac}$ ,  $Y_{ac}$ ) was found using the equations:

$$X_{ac} = 111.12 (\text{aircraft longitude} - \text{radar longitude}) \times \cos (\text{aircraft latitude})$$

$$Y_{ac} = 111.12 (\text{aircraft latitude} - \text{radar latitude}).$$

The longitude and latitude of the aircraft were taken from the INS, and the coordinates for the NSSL Norman Doppler or NASA Wallops SPANDAR radars were tabulated values.

It should be noted that the equations for  $X_{ns}$  and  $Y_{ew}$  compensated for the relative motion of the aircraft during the sample interval by using the instantaneous values of aircraft heading, longitude, and latitude. Therefore, the lightning points plotted in the figures in this paper are located at the true locations as detected by the locator system.

For comparison purposes, the aircraft ground tracks ( $X_{ac}$ ,  $Y_{ac}$ ) were plotted along with the lightning locations ( $X_{ns}$ ,  $Y_{ew}$ ) and the contours of precipitation reflectivity and spectrum width (turbulence).

## NSSL/USAF Aircraft

A U.S. Air Force RF-4C aircraft was operated in a joint USAF/NSSL program to measure turbulence and wind shear within convective storm cells in Oklahoma. The RF-4C is a twin-engine, two-seat, fighter-type aircraft with the structural ruggedness and reserve power necessary for thunderstorm penetrations. A dimensioned three-view drawing of the aircraft is given in figure 3.

The following parameters were recorded by the magnetic tape data system onboard the aircraft: outside air temperature, angle of attack, angle of sideslip, normal acceleration, pressure altitude, stabilator position, radar altitude, airspeed, and magnetic heading. The instrumentation system included an AN/ASN-56 inertial navigation system (INS). The recorded INS parameters were pitch and roll angle, pitch rate, and ground speed and direction. These data were recorded at a sample rate of 21.9 samples/sec. A time code generator synchronized to WWV was used as a time base.

The aircraft track of the NSSL/USAF RF-4C aircraft was established every 20 seconds from the location of the aircraft transponder displayed on the photographically recorded WSR-57 radar plan position indicator (PPI) scope. Linear interpolation was used to position locations between scans. Aircraft and radar data were synchronized using WWV time-based checks. Digitally recorded aircraft data were computer processed and expressed in engineering units.

The vertical winds,  $w$ , in m/sec were computed using:

$$w = V_{ta} \alpha + V_{ta} \beta_a - V_{ta} \theta + \int_0^t a_z dt + w_{p,g}(0) + L_v \dot{\theta}$$

where:

$V_{ta}$  = true air speed (m/sec)

$\alpha$  = angle of attack (rads)

$\beta_a$  = sideslip angle (rads)

$\theta$  = pitch angle (rad)

$a_z$  = aircraft vertical acceleration (m/sec<sup>2</sup>)

$w_{p,g}(0)$  = vertical velocity of the aircraft at time  $T = 0$  (m/sec)

$\dot{\theta}$  = pitch rate (rads/sec)

$L_v$  = distance from accelerometer to angle of attack measurement point (m).

As another measure of turbulence, the derived equivalent gust velocity,  $U_{de}$ , was also used. This value was computed from aircraft recorded data using the general equation (from reference 1):

$$U_{de} = \frac{2W \Delta a_z}{V_e K_g \rho_0 C_{L_\alpha} S_a}$$

where

- $W$  = aircraft weight (N)
- $\Delta a_z$  = measured aircraft incremental vertical acceleration from normal (g units)
- $V_e$  = equivalent airspeed to sea level (m/sec)
- $K_g$  = gust alleviation factor
- $\rho_0$  = air density at sea level ( $\text{kg/m}^3$ )
- $C_{L_\alpha}$  = change in aircraft lift coefficient
- $S_a$  = aircraft wing area ( $\text{m}^2$ )

#### Ground-Based Radars

WSR-57 radar.- The WSR-57 weather surveillance radar is the type used in the National Weather Service network. The radar characteristics were: half-power beam width of  $2.2^\circ$ ; wavelength of 10.6 cm; and peak power of 300 kW. The radar located at Norman, Oklahoma (see figure 4), continuously scanned all azimuth sectors at an  $18^\circ/\text{sec}$  rate to provide a surveillance of all storms within 300 km of Norman. The elevation angle was usually  $0.5^\circ$ . Every 5 min, the elevation angle was stepped in increments of  $2^\circ$  each revolution in order to have storm cross sections at different heights.

The radar's logarithmic receiver output was integrated and then range normalized to produce digital estimates proportional to effective reflectivity factor in dBZ. The digital estimates were quantized in six categories and displayed in a Plan Position Indicator (PPI) manner on a CRT. This PPI display was used during the test operations to help guide the NASA and USAF aircraft to storm cells of interest, and to avoid hazardous weather exceeding the capabilities of the aircraft. An MPX-7/UPX-6 surface-based aircraft transponder interrogator, located adjacent to the WSR-57 radar, provided aircraft position data (out to 400 km) which was superimposed on the WSR-57

radar scope. This display, in conjunction with telephone communications to the appropriate air traffic control centers, was used by an assigned FAA air traffic controller at NSSL to coordinate control of the two test aircraft.

Doppler radars.- A matched pair of Doppler radars, one located at Norman, Oklahoma, and another at Cimarron Airport, Oklahoma City, Oklahoma (see figure 4), are used by the NSSL to scan through storms of interest. During these tests, however, no storms entered the dual Doppler area. In fact, all the Doppler radar data shown in this paper were obtained by the Norman Doppler radar.

A Doppler radar generates a datum of reflectivity factor (a measure of rainfall rate, assuming a Marshall-Palmer distribution of droplets, in dBZ), mean radial velocity to or from the radar (in m/sec), and Doppler radial velocity spectrum width (in m/sec) for each resolution volume. The relationship of reflectivity to rainfall rate and intensity level for a typical WSR-57 weather radar used by the National Weather Service is given in table I. The spectrum width can be interpreted as a measure of turbulence. (Details on the Doppler radar parameters and measurement techniques may be found in references 2 and 3.)

The radar characteristics were: half-power beam width of  $0.81^{\circ}$ ; wavelength of 10.52 cm; and peak power of 750 kW. Typically, the rotation rate was  $6^{\circ}$ /sec. Periodically, the elevation angle was stepped in increments in order to have storm cross section at different heights. For these tests, the radar resolution volume had a  $1^{\circ}$  azimuth extent,  $1^{\circ}$  elevation extent, and 150 m range extent. The first two parameters are fixed values, but the range extent can be varied from 150 m to 1 km.

The Doppler radar reflectivity data are presented in this paper as constant contours on an essentially level plane at the same altitude. Correspondingly, the Doppler spectrum width data, representing turbulence, are presented as constant contours on the same planes. The techniques used for generating this presentation are outlined below.

The reconstruction of the thunderstorms on May 11, 1978, and on June 1, 1978, from the unprocessed Doppler radar tapes consisted of three distinct analysis routines: (a) editing the unprocessed, or raw, data tape; (b) interpolating data to uniformly spaced grids on constant elevation surfaces; and (c) plotting contours of equivalent reflectivity factor (dBZ) and spectrum width (m/sec).

An interlaced sampling collection mode was used in which reflectivity samples were acquired separately from velocity samples. The interlaced sampling mode allowed the resolution of range-ambiguous echoes by identifying the true ranges and strengths of all echoes, and this information was used to unscramble the ranges associated with the velocity data, or to eliminate those data when two or more echoes were overlaid.

For the storms of May 11, and June 1, 1978, the radar sampling parameters produced an unambiguous radar range of 115 km. When range scrambling



was detected at a given range gate, the reflectivity and spectrum width measurements were removed from the data set, although the reflectivity data were not scrambled. Thus, there are regions on the contoured plots where it appears the contours end abruptly.

Reflectivity was computed using the radar equation given in references 4 to 6. The spectrum width was computed using the analysis given by Zrnic<sup>1</sup>.

For small elevation angles ( $\leq 10^\circ$ ), the data on constant elevation surfaces could be displayed on a plane surface with little distortion by interpolating points to a horizontal surface tangent to the radar location. The data were weighted using a Cressman filter (reference 7) applied to a prolate spheroidal interpolation volume. The vertical influence radius was made disproportionately large, keeping the horizontal radius at 1 km, and data used were taken from a single azimuthal scan at one elevation. This procedure caused a small distortion factor, which at  $1^\circ$  elevation, was less than 0.02 percent. Thus, by using only one elevation of data for each run, a contoured simulated PPI plot for the first trip could be constructed. Displaying data at constant elevation angle was more satisfactory than displaying data at constant height because elevation angle spacings used in data acquisition caused too many gaps in data fields at constant height.

Contours of reflectivity factor (dBZ) and spectrum width (m/sec) were created by using a least-squares fit on the 120 km x 120 km data matrix. The computed contour intervals for reflectivity factor were 10, 20, 30, 40, 45, 50, 55, and 60 dBZ. For clarity and simplicity in this paper, these contours were combined to 10-40 dBZ, and greater than 40 dBZ. For spectrum width, the contour intervals were 2, 6, 10, and 14 m/sec. Because of poor spectrum width estimation at low signal-to-noise ratios, the spectrum width at the edges of storms (reflectivity  $\leq 10$  dBZ) should be considered spurious. A good discussion on this problem is given in reference 8.

#### NASA Wallops SPANDAR Radar

As was the case during the NSSL flight tests, contours of constant precipitation reflectivity in dBZ were desired for the single flight in the vicinity of NASA Wallops in Virginia. The radar precipitation reflectivity measurements were made by the S-band research radar (SPANDAR) at NASA Wallops. Unlike the NSSL Doppler radar, however, the SPANDAR radar could not measure spectrum width.

The SPANDAR radar sampled precipitation intensity (reflectivity) at 1- $\mu$ sec intervals out to a maximum range of approximately 75 n.mi. The peak power output was 1 MW, the pulse repetition frequency was 320, the beam width was  $0.4^\circ$ , and the range accuracy was 229 m (750 ft). The raw data tape of radar video was digitized following the flight, and converted to received power and rainfall rate by the radar equations. The final computation step was the correction of rainfall rate for range to give reflectivity in dBZ. The reflectivity values were averaged over surfaces of 1000 m by 1000 m for

---

<sup>1</sup>Zrnic', D. S.: Spectrum Width Calculation. NSSL Memorandum for the Record, Apr. 1978. (Unpublished.)

the PPI plots and over surfaces of 300 m by 300 m for vertical scans, and then plotted at the centers of each averaged area. For simplicity of analysis, the reflectivity values were computer sorted into 5-dBZ increments starting at 20 dBZ for plotting. Finally, the computer plots were further simplified to give contours of 20-30, 30-50, 50-60, and 60-65 dBZ. Details on the SPANDAR radar system and radar computations may be found in reference 9.

## Test Procedures

NSSL.- For all of the test flights made in conjunction with the NSSL, visual flight was maintained by the NASA aircraft, although the aircraft did fly in close proximity to active thunderstorms. The onboard data system recorded lightning activity as measured by the airborne lightning locator system while ground-based radar measurements were made of the same storm. Attempts were made to correlate the pilot visual observation of the storm system with the information provided by the lightning locator system.

The NSSL/USAF aircraft was directed through thunderstorms of interest to gather in-situ turbulence measurements. The aircraft was kept out of areas of precipitation reflectivity which exceeded 45 dBZ.

Air traffic control of the two aircraft was coordinated by a dedicated FAA air traffic controller, using the WSR-57 radar display with the superimposed aircraft transponder positions. The controller, located at NSSL, was in telephone communication with the required air traffic control facilities, and in direct radio contact with both aircraft.

The aircraft flight paths were programmed by the NASA and NSSL researchers, who were co-located with the controller. For assistance in making flight decisions, Doppler radar data were presented in direct view of the controller and researchers. These Doppler data were supplemented by closed-circuit television presentation of the latest weather satellite picture covering the area.

NASA Langley.- Following the flight test program at NSSL, the NASA aircraft returned to NASA Langley for test flights over the Chesapeake Bay during August 1978. Unlike at NSSL, the NASA aircraft penetrated a small, isolated cumulonimbus cloud which showed no electrical activity on the airborne lightning locator. The aircraft crew maintained radio communications with the local air traffic control facilities and the Flight Service Office at NASA Langley. The aircraft crew was also in radio communication with the SPANDAR radar site at NASA Wallops. Because of the limited nature of the real-time displays at the SPANDAR site, however, the NASA flight crew programmed their own flight paths. As was the case at NSSL, records were made of the airborne lightning locator system while ground-based radar measurements were made of the same storm (by the SPANDAR radar).

## DISCUSSION OF RESULTS

During the 1978 storm season, a total of 14 storms were surveyed with the combined airborne data and ground-based data systems. Thirteen storms were studied in the vicinity of NSSL at Norman, Oklahoma, and one storm was studied in the vicinity of NASA Wallops in Virginia. An appreciable amount of lightning activity was measured during twelve of these storms. However, for two storms, very little lightning activity was measured or reported, yet the other hazard measurements indicated significant levels of reflectivity and turbulence. The following discussion gives typical details for storms representing these conditions. The storm of June 1, 1978, at Norman, Oklahoma, represents the general case with appreciable lightning activity, and the storms of May 11, 1978, at Norman and August 14, 1978, at NASA Wallops represent the less general case of very little lightning activity.

### 1978 Storm Hazards Research

Storm of June 1, 1978, at Norman, Oklahoma. - An area of scattered heavy thunderstorms formed in central Oklahoma to the north and east-southeast of Norman at 15:12 CST. The storms to the north of Norman formed a line about 50 km long. This line moved slowly to the east, with individual cells in the line propagating from  $250^{\circ}$  at 7 m/sec. The storms to the southeast of Norman moved from  $240^{\circ}$  at about 9 m/sec. The maximum heights of these storms never exceed 13.1 km (43 000 ft).

The airborne lightning locator system was operated and recorded continuously from 15:11:50 to 15:59:30 CST. The rate of production of lightning points detected by the airborne locator is plotted as a function of time in Figure 5, along with the start and stop times of the four Doppler radar data sample periods. The lightning events occurred at a rate more than 1 every 2 secs for most of the data period, with a peak rate of 2.4 points/sec at 15:32:16 CST. Interestingly, at 15:26 CST, the storm to the southeast seemed to intensify, while the strength of the storms to the north remained unchanged. All the storms in the area weakened in intensity from 15:41 CST until 16:00 CST. There was a corresponding decrease in lightning activity between 15:40 and 15:50 CST. However, for each of the four Doppler radar sample periods, the peak reflectivity and spectrum width values in the cells being studied were 45 dBZ and 6 m/sec, respectively.

The reflectivity contour data taken during the third Doppler radar data interval (15:41:34 - 15:46:39 CST) are given in Figure 6 for discussion of this storm as the activity is typical of the storm as a whole. A typical presentation from the airborne lightning locator during this time interval is given in Figure 7. The 74 points displayed were those contained within the system memory at 15:42:52 CST. These points had been accumulating (190 secs) since the last clear at 15:39:32 CST. New lightning points were being detected at a rate of 0.1333 points/sec over the 30-second period from 15:42:37 to 15:43:07 CST. The lightning activity was concentrated at the 2 o'clock and 5 o'clock positions at a range of 40 n.mi. This airborne display would indicate that a path to the left of the current course would avoid lightning activity.

All of the lightning points detected during the entire third Doppler radar data period are shown plotted in their true positions with respect to the Norman Doppler radar in figure 6 along with the NASA aircraft ground track during this period. The aircraft was flying to the northwest, south of several storm cells with peak reflectivities of 40 and 45 dBZ. Several storm cells of similar reflectivity levels were located to the southeast of the aircraft. Reflectivities of 45 dBZ indicate a high probability of hail within the 45 dBZ contour, and a good chance of encountering moderate turbulence somewhere within the storm cell. The relative bearings of the lightning points to the aircraft are generally the same as the relative bearings of the Doppler radar reflectivity contours to the aircraft. However, many of the measured lightning locations are shown at a greater range from the aircraft than the Doppler radar reflectivity contours.

The same measured lightning locations and aircraft ground track are shown in figure 8 with the Doppler radar spectrum width contours for the same data interval. The various storm cells contain spectrum width values ranging from 2 to 6 m/sec, corresponding to light turbulence (reference 10). As was the case with the data in figure 6, the lightning locations have the same general bearing with respect to the aircraft as the Doppler radar contours, but are also shown to be further from the aircraft than the Doppler radar contours. For this typical, electrically active thunderstorm system it can be said that the airborne lightning locator data agreed generally with the location of the most severe weather as indicated by the NSSL ground-based Doppler radar. For this storm system, the airborne lightning locator system gave sufficient information to avoid the areas of high reflectivity (precipitation) and spectrum width (turbulence).

Storm of May 11, 1978, at Norman, Oklahoma.- A line of severe thunderstorms with pea-sized hail propagated from south-central Oklahoma to the east at 7 m/sec late in the afternoon of May 11, 1978. This line extended from Duncan, Oklahoma, to 40 km southwest of Archer City, Texas. Individual cells in this line moved at 16 m/sec from 250° during four Doppler radar data collection periods from 16:23:14 to 16:52:43 CST.

Very low rates of lightning production occurred throughout this storm. Unfortunately, the significance of this fact did not become apparent until after the flight was over. The aircraft had already taken 20 mins of data earlier in the flight in the vicinity of Ponca City, Oklahoma. In order to conserve the remainder of the data recorder tape, periods of little electrical activity were not recorded, although the airborne lightning locator system was in continuous operation throughout the flight. However, data were recorded for four short intervals when the aircraft was headed towards 40-dBZ reflectivity contours to document the lack of lightning activity. The crew noted that the low level of activity was no different during the recorded periods than during the non-recorded periods.

The rate of production of lightning points detected by the airborne lightning locator system is plotted as a function of time in Figure 9 along with the start and stop times of the four Doppler radar data sample periods. The start and stop times of the single penetration by the NSSL/USAF aircraft

are also plotted in figure 9. The maximum lightning production rate for this storm was only 0.0666 points/sec. The low level of activity did not change with variations in the intensity of the storm. The peak reflectivity dropped from 50-55 dBZ during the first Doppler radar interval to 40-45 dBZ during the fourth interval. High spectrum widths (greater than or equal to 10 m/sec) were observed near the core of the storm during the first, second, and fourth Doppler radar period. The maximum height of the southern-most cell under study decreased from 14.6 km (48 000 ft) at 16:10 CST to 14 km (46 000 ft) at 16:45 CST with no corresponding change in lightning activity.

The data from the fourth Doppler radar period (16:47:30 to 16:52:43 CST) were chosen for discussion because this was the only time that both airborne lightning locator data and in-situ turbulence data from the NSSL/USAF aircraft were available. A typical presentation from the airborne lightning locator system during part of the fourth interval is given in figure 10. At 16:48:09 CST, only two points were being displayed ahead of the aircraft at 40 n.mi. range. These two points had been accumulating since 16:47:40 CST, when the data recording system was turned on. The rate of production was only 0.0416 points/sec over the 24-second period from 16:47:52 to 16:48:16 CST.

The four lightning points detected during the entire fourth Doppler radar data period are shown in figure 11 along with the Doppler radar reflectivity contours and ground tracks of the NASA and NSSL/USAF aircraft with respect to the Norman Doppler radar. A similar presentation with respect to the Doppler radar spectrum width contours is given in figure 12. As was the case for the comparisons for the June 1, 1978, storm (figures 6 and 8), the airborne lightning locator data agreed with the general locations of the most severe weather, as indicated by the NSSL ground-based Doppler radar. For the storms studied in this program, when comparing lightning locations from the airborne lightning locator system with ground-based Doppler radar measurements of reflectivity and spectrum width, the airborne lightning locator system data points tended to be further from the aircraft position than the Doppler radar contours, but at the same relative bearing from the aircraft as the Doppler contours.

The actual turbulence occurring inside the storm was measured by the NSSL/USAF aircraft from 16:47:13.4 to 16:50:53.4 CST during a storm penetration from northwest to southeast at a nominal altitude of 6.1 km (20 000 ft). Time histories of maximum derived equivalent gust velocity ( $U_{de}$ ) and vertical gust velocity computed from the onboard instrumentation are shown in figure 13. The reflectivity intensity through which the aircraft was flying is also plotted in figure 13 for reference, where these reflectivity values were taken from a reflectivity contour plot interpolated to a constant altitude of 0.3 km. The peak  $U_{de}$  values ranged from 7 to 9 m/sec, corresponding to a moderate level of turbulence (reference 10). During the penetration, the pilot reported moderate turbulence at 16:48:46 and 16:49:03 CST. Vertical gust velocities of  $\pm 9$  m/sec were experienced during this time period. In summary, the storm of May 11, 1978, was an intense convective storm which generated little or no lightning for a significant part of its life cycle, but produced at least moderate turbulence. The airborne lightning locator system gave much

less indication of lightning activity during this storm than during other storms which had similar Doppler radar contour levels of reflectivity and spectrum width. This calls into question the relationship of lightning to other measures of severe storm hazards.

Storm of August 14, 1978, at NASA Wallops.- The fourteenth, and final, storm of the 1978 storm season occurred over the Chesapeake Bay, on August 14, 1978. The research flight was made in conjunction with ground-based measurements of precipitation reflectivity by the S-band SPANDAR radar at NASA Wallops.

The rate of production of lightning points detected by the airborne lightning locator system is plotted as a function of time in figure 14, along with the times during which the four SPANDAR radar scans were made. As was the case with the Oklahoma thunderstorm of May 11, 1978, very little lightning activity was measured during the storm. The output of the airborne lightning locator system was recorded during four intervals to document the lack of activity. Although the recording system was not operated continuously, close visual observation by the crew indicated that there were no lightning events during the periods when the recorder was not operating.

During the third recording period of the airborne lightning locator system (20:10:45 to 20:16:30 GMT), the NASA aircraft penetrated what visually appeared to be a benign storm. The aircraft ground track is shown on the precipitation reflectivity contours from the SPANDAR radar scan made starting at 20:01:20.7 GMT, in figure 15. The SPANDAR radar detected a peak reflectivity of 60-65 dBZ. The maximum top of 9.1 km (30 000 ft) was detected along the 325° azimuth at 20:26:57.1 GMT; a lower top of 8.8 km (29 000 ft) was found at 20:15:04 GMT along the 320° azimuth. During the entire data run shown in figure 15, only one lightning event was detected in the vicinity of the storm contours, and is plotted in its true relative position with respect to the NASA Wallops SPANDAR radar in figure 15. Two other lightning points were recorded during the run, but both were located outside the plotted region in areas of clear air.

As the aircraft flew deeper into the storm cell, the turbulence began to increase and the rain became very heavy. The pilot executed a 90° turn to depart the storm because of the worsening conditions. The turn was apparently made when the aircraft was in an area with a reflectivity between 55 and 60 dBZ (see figure 15). A peak vertical acceleration of 0.7 g incremental was recorded at 20:12:45.7 GMT, while the aircraft was turning. This vertical acceleration peak is equivalent to a  $U_{de}$  of 5.4 m/sec (17.7 ft/sec), which is near the threshold of moderate turbulence (reference 10). The high reflectivity values were probably due to the large quantity of low altitude moisture in the atmosphere over the Chesapeake Bay, rather than by hail, as is typically the case in Oklahoma thunderstorms. (There is a slight possibility that the aircraft flew through a lower reflectivity region because of motion of the storm in the time between the radar sample and the penetration, and the difference in altitude between the aircraft altitude and the height of the radar sample.)

Of the fourteen storms studied, two storms (May 11, 1978, in Oklahoma, and August 14, 1978, in Virginia) had little lightning activity but heavy precipitation and moderate turbulence. Apparently, there are some convective storms which generate little or no lightning for a significant part of their life cycle, but can produce at least moderate turbulence. Therefore, a lack of lightning cannot be accepted as an inference of a corresponding lack of other hazards to the flight of aircraft through convective storms.

#### Further Storm Hazards Research

The NASA Storm Hazards Research Program did not conclude with the 1978 flight tests. During 1979, a NASA-owned F-106B aircraft was flown on the peripheries of thunderstorms in the vicinity of NASA Wallops to gain operational experience prior to actual thunderstorm penetration flights. A report on the 1979 operations is given in reference 11.

During the 1980 storm season, the F-106B made approximately 70 thunderstorm penetrations during 20 storm flights in the vicinity of NSSL and NASA Wallops. During these penetrations, the aircraft sustained 10 direct lightning strikes, whose electromagnetic properties were measured by an onboard direct-strike lightning instrumentation system described in references 11 and 12. The preliminary results from this system are given in references 13 and 14.

The flight experiments carried onboard during the 1980 mission were:

lightning related

direct-strike lightning

lightning data logger (in cooperation with Boeing)

atmospheric chemistry (air sampler for  $N_2O$ )

lightning X-rays (University of Washington)

composite fin cap

non-lightning related

turbulence

wind shear

storm hazards correlation.

A schematic of the mission operations with the F-106B aircraft in the vicinity of NASA Wallops is given in figure 16. This schematic shows the

general layout of the experimental packages in the aircraft and the ground-based data systems which are used. It should be noted that the WSR-57 radar is located at Patuxent River, Maryland, and the radar image is transmitted by telephone line to a color television monitor in the SPANDAR radar control room. A description of the NASA Wallops instrumentation is given in a paper reference 15.

During the 1979 and 1980 storm seasons, the airborne lightning locator system was installed in the F-106B, and was used by the flight crew as a real-time guide to determine the most electrically active storm cell for penetration. Flight tests with the F-106B will continue through the 1983 storm season. During these operations, comparisons of the output of the airborne lightning locator system in the F-106B and from another locator installed at the SPANDAR radar control site will be made with the output of the lightning direction and ranging system shown in figure 16.

#### SUMMARY OF 1978 TEST RESULTS

NASA Langley Research Center has undertaken a storm hazards program to extend the knowledge and understanding of atmospheric processes as they affect aircraft design and operations. The initial phase of this program, conducted during the storm season of 1978 at NSSL and NASA Wallops, involved flight tests around the periphery of storms using a NASA-owned light transport aircraft equipped with a commercially available airborne lightning locator system. The results of the comparison between airborne indications of lightning and other measurements of storm hazards are:

1. There are some convective storms which generate little or no lightning for a significant part of their life cycle, but can produce at least moderate turbulence. Therefore, a lack of lightning activity cannot be accepted as an inference of a corresponding lack of other hazards to the flight of aircraft through convective storms.
2. The airborne lightning locator system data agreed generally with the location of the most severe weather as indicated by the NSSL ground-based Doppler radar. When comparing lightning locations from the airborne lightning locator system with ground-based Doppler radar measurements of reflectivity and spectrum width, the lightning locations tended to be further from the aircraft position than the Doppler radar contours, but at the same relative bearing from the aircraft as the Doppler radar contours.

#### ACKNOWLEDGEMENTS

The author would like to acknowledge the contributions of the staff of the National Severe Storms Laboratory in preparing the Doppler radar contours shown in this paper and in providing the descriptions of the WSR-57 and Doppler radar systems. In particular, the author would like to thank Mr. Jean T. Lee, Dr. Richard J. Doviak, and Mr. Steve Goodman.



## REFERENCES

1. Pratt, Kermit G.; and Walker, Walter G.: A Revised Gust-Load Formula and a Reevaluation of VG Data Taken on Civil Transport Airplanes from 1933 to 1950. NACA Report 1206, 1954.
2. Albery, R.; Weaver, J.; Sirmans D.; Dooley, J.; and Bumgarner, B.: Spring Program 76, Section II, NOAA Technical Memorandum ERL NSSL-83, pp. 79-130, 1977.
3. Lee, J. T.: Application of Doppler Weather Radar to Turbulence Measurements Which Affect Aircraft. FAA Report No. FAA-RD-77-145, March 1977.
4. Probert-Jones, J. R.: The Radar Equation in Meteorology, Quarterly Journal of the Royal Meteorological Society, Vol 88, pp. 485-495, 1962.
5. Doviak, R. J.; and Zrnic', D.: The Weather Radar Equation-Receiver Bandwidth Considerations. Preprints, 18th Conference on Radar Meteorology, American Meteorological Society, pp. 484-489, March 28 and 31, 1978.
6. Berger, Myron I.: A Dual Doppler Radar Investigation of Planetary Boundary Layer Winds in the Optically Clear Atmosphere. Master Science Thesis, University of Oklahoma, pp. 64-65, 1978.
7. Cressman, G. P.: An Operational Objective Analysis System. Monthly Weather Review, 87, pp. 367-374, 1959.
8. Sirmans, D.; Zrnic', D. S.; and Bumgarner, W.: Estimation of Maximum Unambiguous Doppler Velocities by Use of Two Sampling Rates. 17th Conference on Radar Meteorology, American Meteorological Society, pp. 23-28, October 1978.
9. Konrad, T. G.; and Kropfli, R. A.: Radar Derived Spatial Statistics of Summer Rain, Volume II - Data Reduction and Analysis. NASA CR-2592, September 1975.
10. Anon.: National Weather Service Operations Manual, Part D, Chapter 22, 1976.
11. Fisher, Bruce D.; Keyser, Gerald L., Jr.; Deal, Perry L.; Thomas, Mitchell E.; and Pitts, Felix L.: Storm Hazards '79 -- F-106B Operations Summary. NASA TM-81779, March 1980.

12. Pitts, F. L.; Thomas, R. M.; Zaepfel, K. P.; Thomas, M. E.; and Campbell, R. E.: In-Flight Lightning Characteristics Measurement System. Presented at FAA-Florida Institute of Technology Workshop on Grounding and Lightning Technology, Melbourne, Florida, March 1979. FAA-RD-79-6.
13. Pitts, Felix L.; and Thomas, Mitchel E.: Initial Direct-Strike Lightning Data. NASA TM-81867, August 1980.
14. Pitts, Felix L.; and Thomas, Mitchel E.: In-Flight Direct-Lightning Research. 1980 Aircraft Safety and Operating Problems, NASA CP-2170, 1981. (Paper 20 of this compilation.)
15. Carr, Robert E.; and Gerlach, John C.: Wallops Severe Storms Measurement Capability. 1980 Aircraft Safety and Operating Problems, NASA CP-2170, 1981. (Paper 15 of this compilation.)

TABLE I.- WSR-57 WEATHER RADAR REFLECTIVITY CHART

Level	Intensity Category	Radar Color	Maximum reflectivity, dBZ	Rainfall Rate		
				Stratiform mm/hr	Convective	
					in/hr	mm/hr
	No precipitation	White	103.5 dBm at zero range	0.0	0.0	0.0
1	Weak	Gray	30	2.54	0.1	5.08
2	Moderate	Black	41	12.7	0.5	27.9
3	Strong	White	46	25.4	1.0	55.9
4	Very Strong	Gray	50			114.3
5	Intense	Black	57			180.3
6	Extreme	White				>180.3

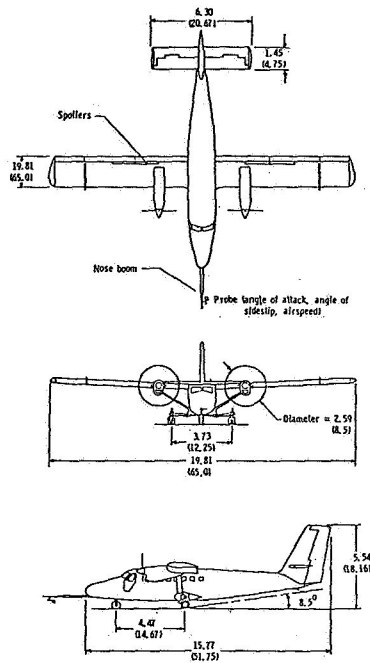


Figure 1.- Three-view drawing of NASA test airplane. All dimensions are in meters (feet).

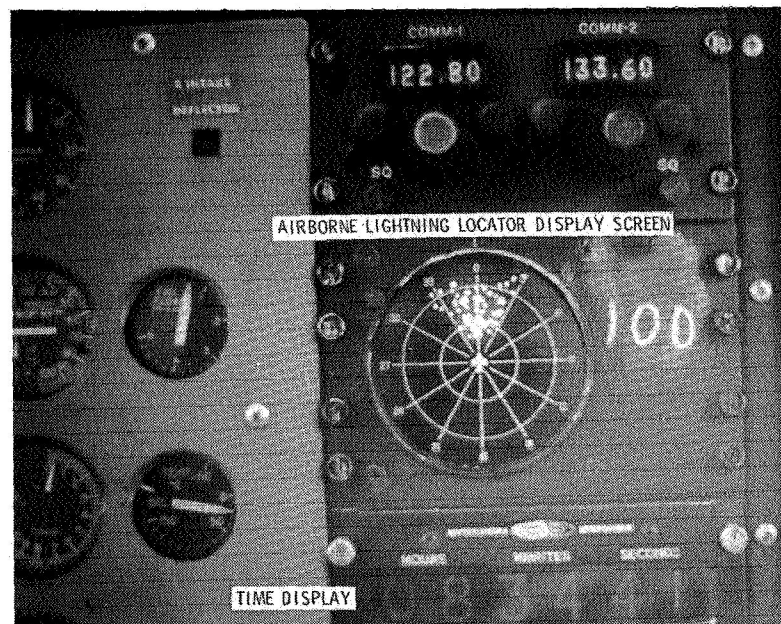


Figure 2.- Airborne lightning locator display in NASA aircraft.

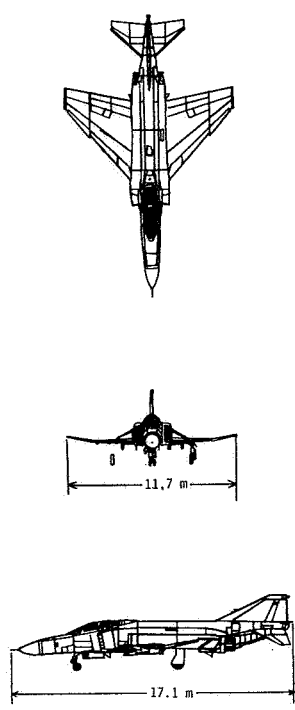


Figure 3.- Three-view drawing of U.S. Air Force RF-4C aircraft flown for NSSL.

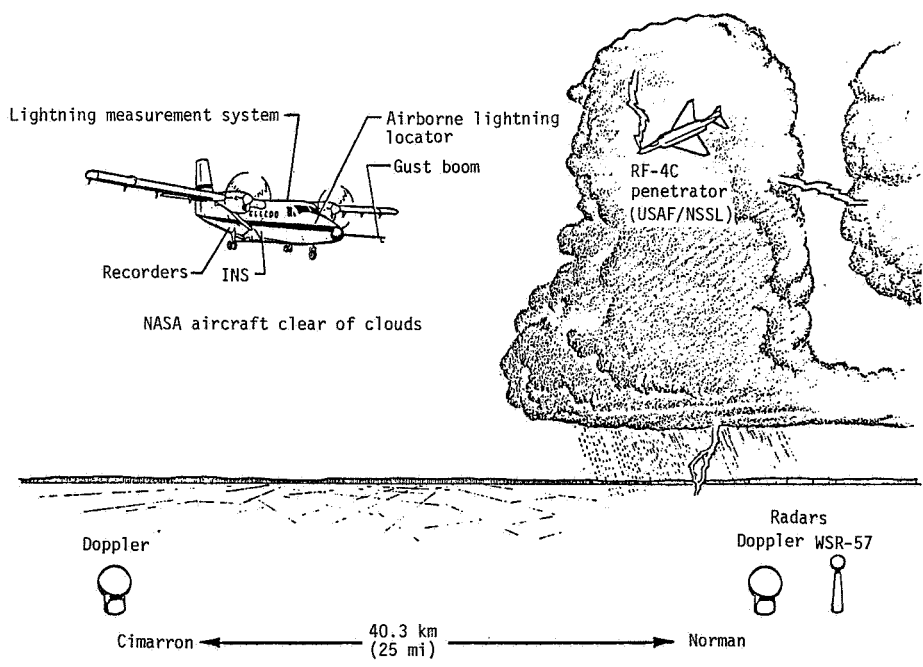


Figure 4.- Schematic of test program at National Severe Storms Laboratory during May 1978.

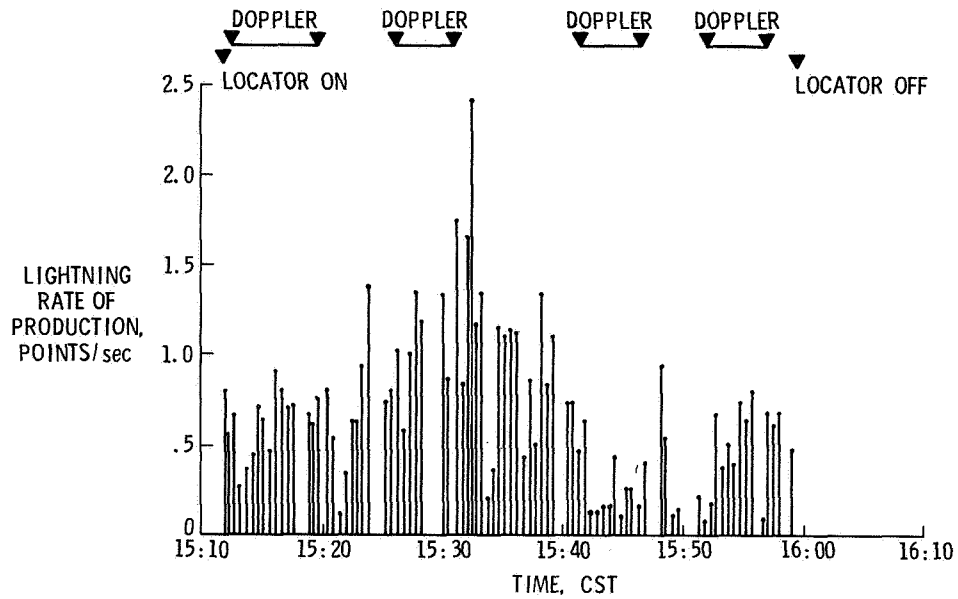


Figure 5.- Rate of production of lightning measured by airborne lightning locator system for storm of June 1, 1978.

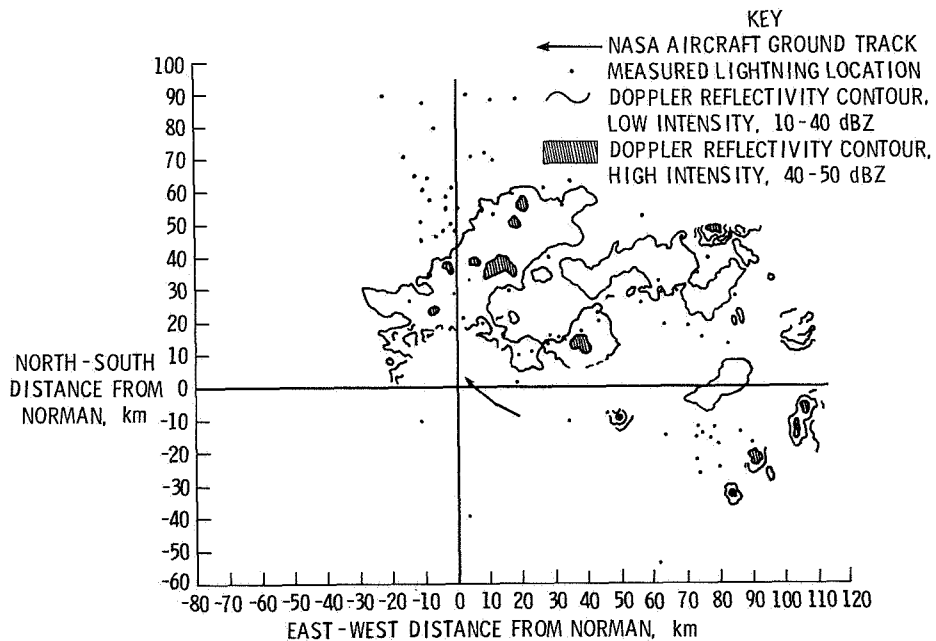


Figure 6.- Doppler radar reflectivity contours and airborne lightning locator points for third Doppler data period (15:41:34 to 15:46:39 CST) on June 1, 1978. Radar angle of  $0.8^\circ$ . Locator range = 40 n. mi.

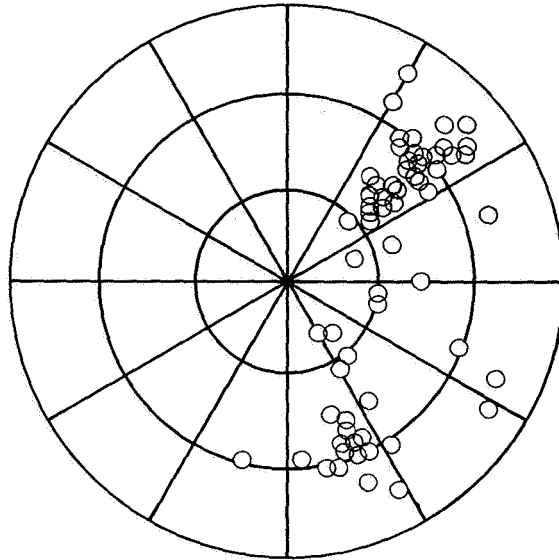


Figure 7.- Airborne lightning locator display at 15:42:52 CST, on June 1, 1978; 40 n. mi. range setting. Rate of production of 0.133 points/sec, 74 points displayed.

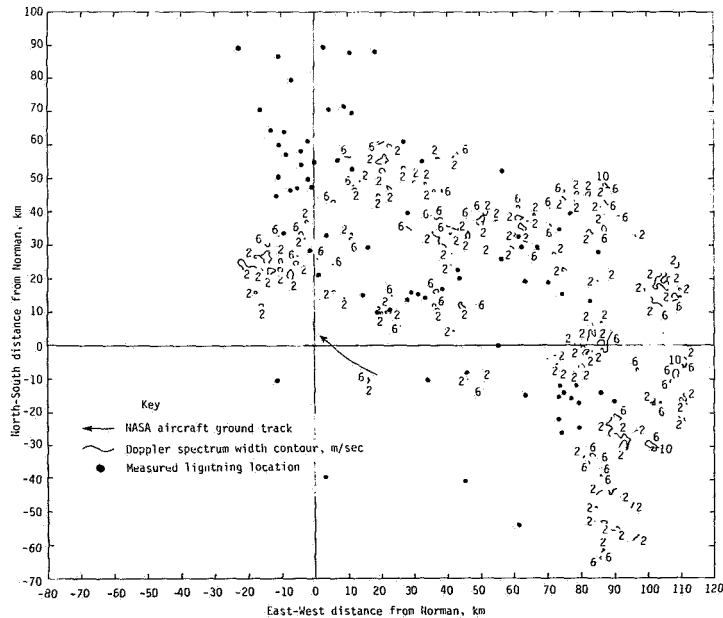


Figure 8.- Doppler radar spectrum width contours and airborne lightning locator points for third Doppler data period (15:41:34 to 15:46:39 CST) on June 1, 1978. Radar angle =  $0.8^\circ$ . Locator range = 40 n. mi.

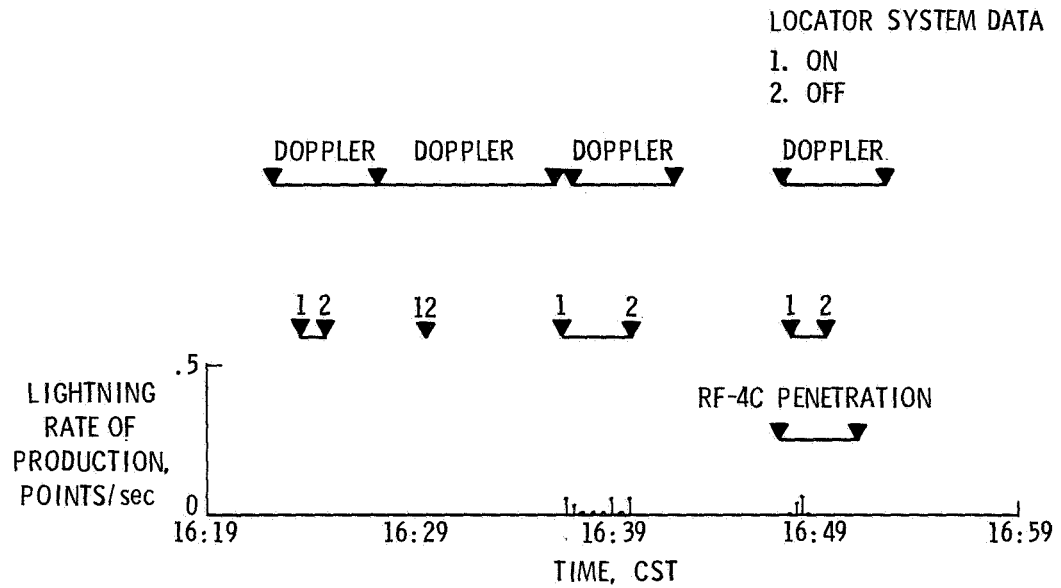


Figure 9.- Rate of production of lightning measured by airborne lightning locator system for storm of May 11, 1978.

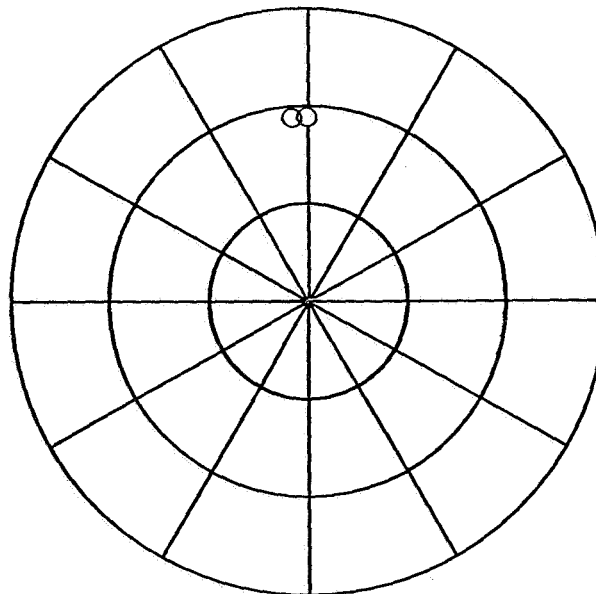


Figure 10.- Airborne lightning locator display at 16:48:09 CST on May 11, 1978; 40 n. mi. range setting. Rate of production of 0.0416 points/sec, 2 points displayed.



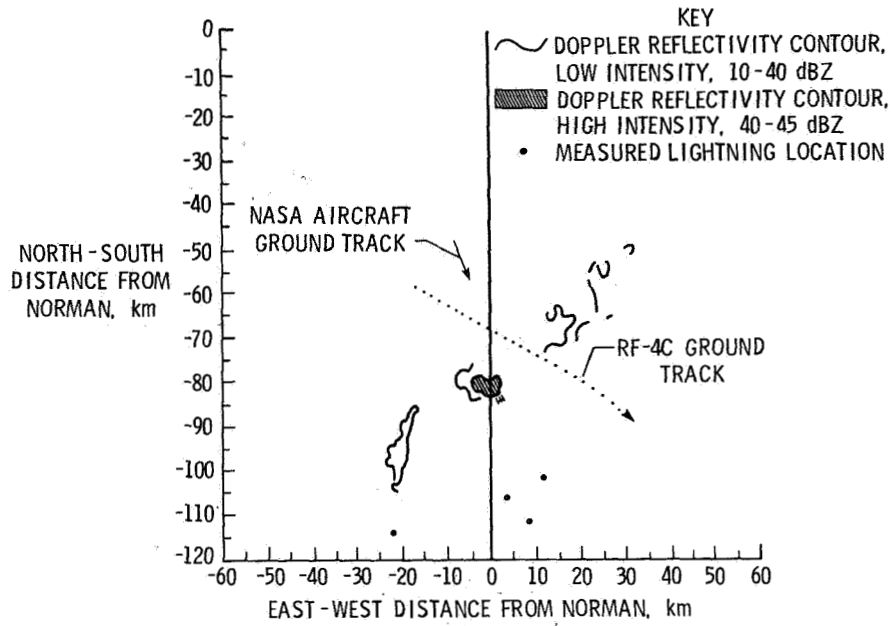


Figure 11.- Doppler radar reflectivity contours and airborne lightning locator points for fourth Doppler data period (16:43:30 to 16:52:43 CST) on May 11, 1978. Radar angle =  $0.6^\circ$ . Locator range = 40 n. mi.

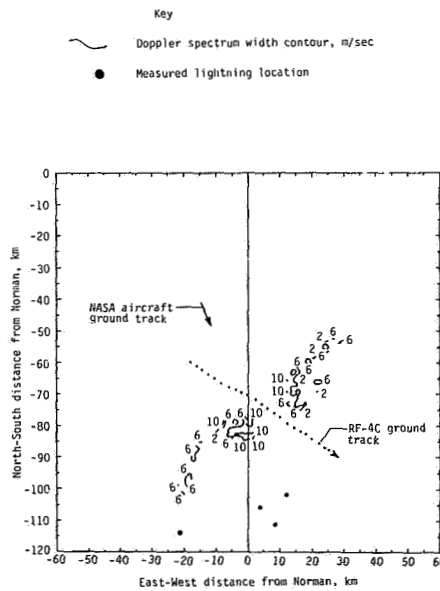


Figure 12.- Doppler radar spectrum width contours and airborne lightning locator points for fourth Doppler data period (16:43:30 to 16:52:43 CST) on May 11, 1978. Radar angle =  $0.6^\circ$ . Locator range = 40 n. mi.

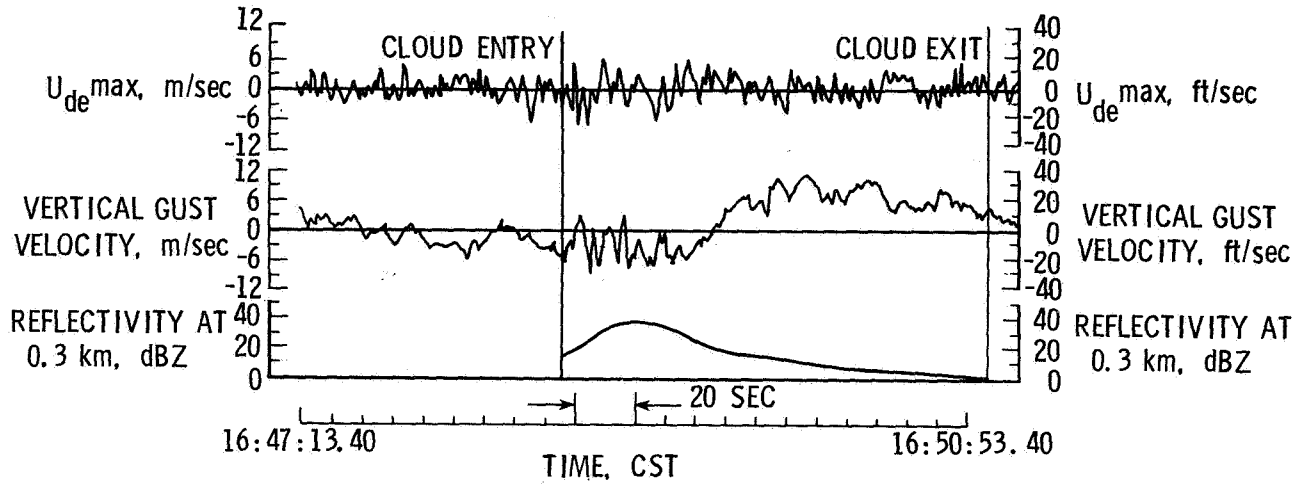


Figure 13.- Airborne turbulence measurements from NSSL/USAF aircraft and radar reflectivity along track during May 11, 1978. Nominal altitude of 6.1 km (20 000 ft) and heading of 110°.

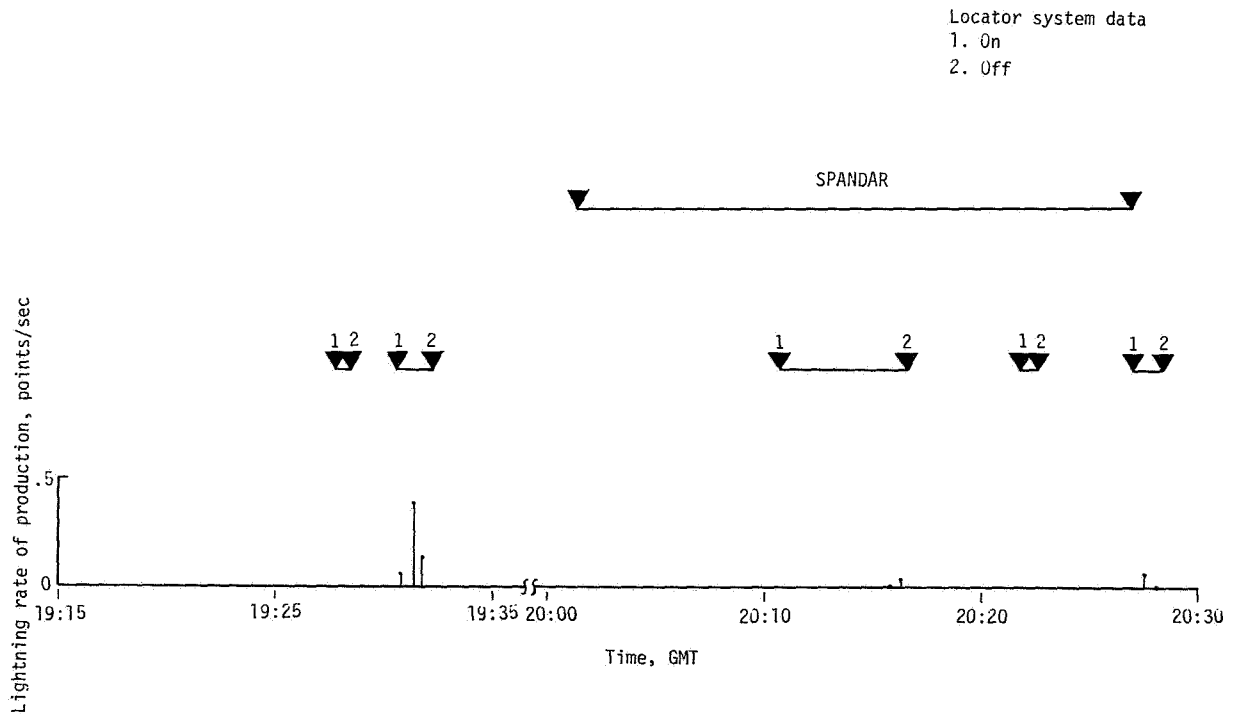


Figure 14.- Rate of production of lightning measured by airborne lightning locator system for storm of August 14, 1978.

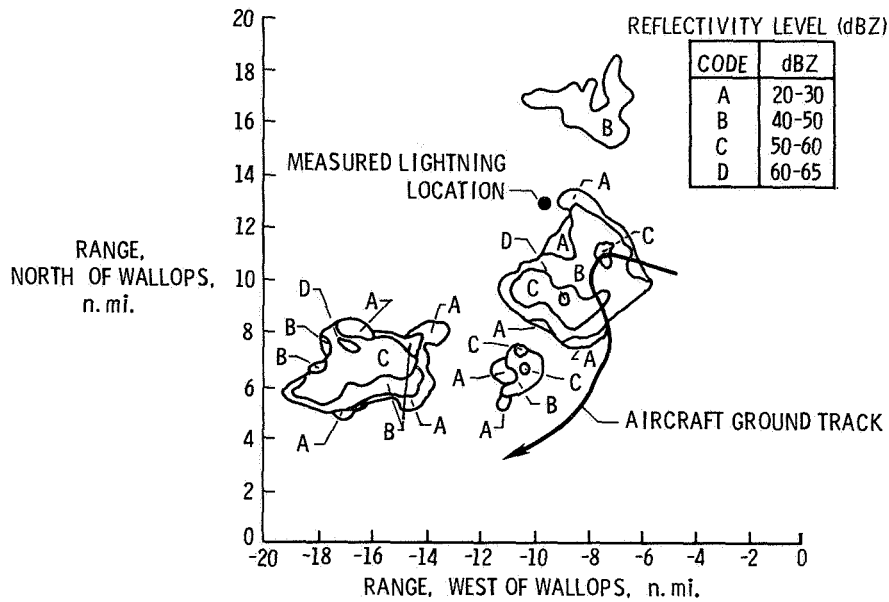


Figure 15.- SPANDAR radar reflectivity contours and airborne lightning locator point for third locator sample interval (20:10:45 to 20:16:30 GMT) on August 14, 1978. Reflectivity recorded at 20:01:20.7 GMT, elevation angle of 0.38 deg. Locator range = 40 n. mi.

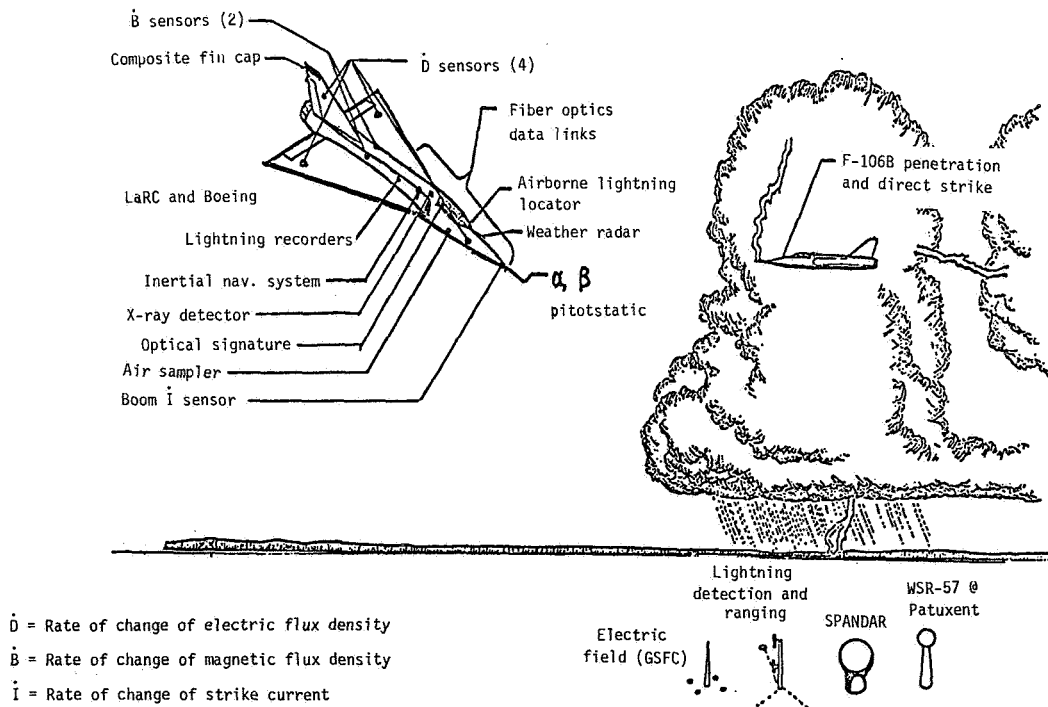


Figure 16.- Schematic of storm hazards mission operations in vicinity of NASA-Wallops.